An Adjustable Microwave Delay Equalizer

KENNETH WOO, MEMBER, IEEE

Abstract—An adjustable microwave delay equalizer is described and the feasibility of using it to provide large amounts of delay over a wide band around 11.2 Gc/s is demonstrated.

The equalizer is composed of a metallic rod slanted in a circular waveguide which is fed at one end with a shunt tee connection to incoming rectangular waveguide.

An experimental model 1.5 m long provides a linear delay of the order of 45 ns over the 680-Mc/s band from 10.80 to 11.48 Gc/s. The bandwidth, center frequency, and shape of delay characteristic are all adjustable.

A similar model can be used for equalization at other frequencies. Theoretical estimation shows that at 6 Gc/s a total delay of 24 ns over a band of 1.2 Gc/s may be achieved with a structure 1 m long.

I. Introduction

IT IS WELL KNOWN that waveguides are dispersive. When a broadband signal propagates in a proposed 35 to 75 Gc/s, TE_{01} mode, 2-inch circular wave-guide system [1], the lower frequency components, travelling at a slower group velocity, will experience more delay than the higher frequency components. Consequently, a pulse propagating from one repeater to the next will become seriously distorted upon travelling through the long section of waveguide between them. For operation of such a system, the use of delay equalizers in each repeater is therefore essential. Different frequency channels in each section of guide require different equalizations. Even the same channel in different sections of guide may need different corrections considering that the distances between repeaters may vary due to geographical requirements. Hence, it is desirable and convenient to have a basic type of equalizer capable of providing various delay compensations.

One way to achieve delay equalization is by means of reflecting energy in a tapered waveguide section whose cutoff frequency increases progressively from the entrance (large end) to the constricted end. This method was suggested by Pierce [2] and later studied extensively by Albersheim, Fisher, Szentirmai, and Tang [3]. It utilizes the fact that a wave propagating in such a waveguide taper will be reflected mostly at the cross section where the cutoff frequency of the taper becomes equal to the wave frequency. When a broadband signal is applied, the higher frequency components will penetrate deeper into the taper and hence have experienced more delay than the lower frequency components upon returning to the entrance. The variation of delay with respect to frequency is thus a reverse of that in a uniform waveguide. Accordingly, a taper can be used to equalize the delay distortion introduced by the section of waveguide between adjacent repeaters provided that the shape (mechanical profile) of the taper is properly designed. Figure 1 shows a circuit, first suggested by Mumford [4], illustrating a simple way to incorporate such an equalizer for use in the waveguide system by utilizing a circulator. The equalizer is connected to port 2 of the circulator. The incoming distorted pulse is introduced into the equalizer through port 1 of the circulator. The equalizer selectively delays the various frequency components and reflects them back through port 3 of the circulator. This circuit can easily be adapted in each repeater at the proposed 11.2 Gc/s IF.

However, the utilization of a physically tapered waveguide to reflect energy for accomplishing delay equalization has certain basic disadvantages. It requires the fabrication of a taper with an extremely high degree of dimensional accuracy. Furthermore, it does not permit any readjustment of the delay vs. frequency characteristic once the taper is made. To overcome these difficulties, this paper introduces a new type of equalizer structure in which cutoff reflections are achieved not in a physically tapered waveguide but in a simulated taper obtained by providing a continuous perturbation along the interior of an otherwise uniform waveguide. The presence of the perturbation in the guide alters the effective electrical cross section (or the cutoff frequency) of the waveguide. By varying the position or the size of the perturbation, the structure can therefore simulate tapers of different shapes. The experimental model to be described here achieves cutoff reflections by perturbing a circular guide with a thin metallic rod. Theoretical and measured results show that large amounts of delay over wide bands are obtainable and that the bandwidth, center frequency and shape of delay characteristic are all adjustable.

II. Theory of Operation

Referring to Fig. 2, the equalizer is composed of a thin metallic rod slanted in the interior of an otherwise uniform hollow circular waveguide. For the TE_{11} mode operation, the rod must be placed in the plane of symmetry in order to avoid conversion from the TE_{11} to the TEM mode. The plane of symmetry is defined as the plane which contains the axis of the guide and is everywhere perpendicular to the electric field lines.

Manuscript received August 31, 1964; revised December 16, 1964.
The author is with Bell Telephone Labs., Inc., Holmdel, N. J.

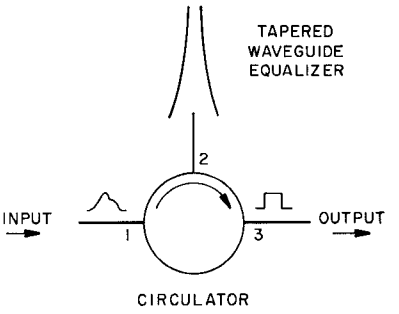

Fig. 1. A delay equalizer circuit.

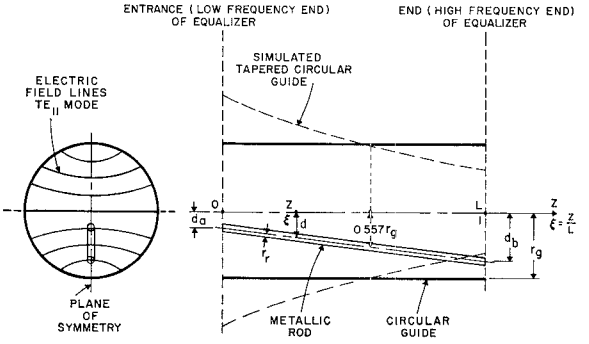

Fig. 2. Schematic of slanted-rod delay equalizer.

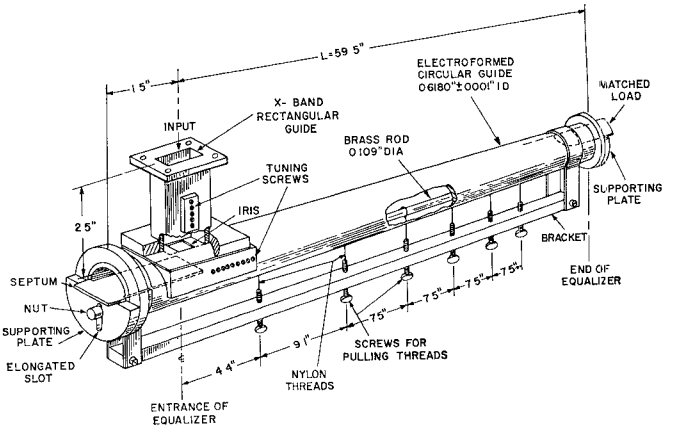

Fig. 3. Experimental model of slanted-rod delay equalizer.

Perturbation theory (see Appendix I) predicts that when a thin metallic rod is in the plane of symmetry and parallel to the axis of a circular waveguide propagating the TE_{11} mode, the following will result:

1) The effective cross section of the structure remains the same as that of the unperturbed guide if the rod is located at a position 0.557 of the guide radius from the center of the guide.
2) The effective cross section becomes gradually larger than that of the unperturbed guide if the rod is moved away from that position toward the center of the guide.
3) The effective cross section becomes gradually smaller than that of the unperturbed guide if the rod is moved away from that position toward the wall of the guide.

Consequently, when the rod is slanted in a general direction from the center toward the wall of the guide as shown in Fig. 2, the structure simulates a tapered circular waveguide with its cross section varying from that larger than to that smaller than the cross section of the unperturbed guide.

As is readily seen, the shape of the taper thus obtained can easily be varied either by slanting the rod in a different orientation or by deflecting the axis of the rod. The delay characteristic of this type of equalizer is therefore inherently adjustable.

III. Experimental Model

The assembly of the experimental model is shown in Fig. 3. The electroformed circular guide is 61 inches long and 0.618 inch $\pm$ 0.0001 inch ID. The cutoff frequency of the guide is 11.2 Gc/s. The commercial brass rod is 0.109 inch in diameter. The ratio of the rod radius to the guide radius is thus equal to 0.176. The equalizer is fed at one end with a shunt tee connection to incoming X band rectangular guide and is terminated at the other end by a matched load. The design of the input junction will be discussed in Section IV.

The rod is supported in the circular guide by means of two end plates attached to the guide. The supporting plates are each provided with an elongated slot through which the ends of the rod pass. The slots are so aligned that the rod is allowed to vary its orientation only in the plane of symmetry. The rod is threaded at each end and, hence, may be stretched and locked in a given orientation by using two nuts. When the rod is locked, its axis may be deflected in the plane of symmetry by pulling nylon threads attached to it at locations spaced along its length as shown. Each thread passes through a small hole in the wall of the guide in the plane of symmetry

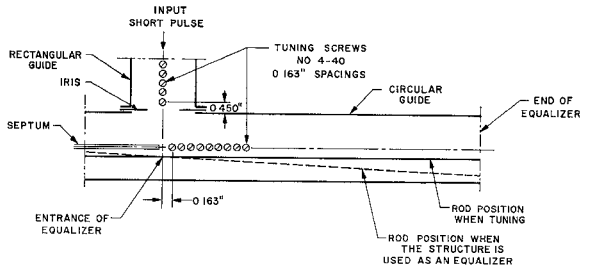

Fig. 4. Input junction tuning setup.

and is fastened to a screw mounted on a bracket. By turning the screws, the rod can be pulled at different locations in varying amounts. The presence of the elongated slots and the nylon threads permits the adjustments of the rod orientation and the rod axis, and thereby the delay characteristic of the equalizer whenever desired.

IV. Input Junction

The input junction couples the TE_{10} wave mode in the incoming X band rectangular guide (0.400 inch by 0.900 inch) into the TE_{11} wave mode in the circular guide of the equalizer. It consists of an iris, a septum, and fourteen tuning screws as shown in Fig. 3. The iris provides a symmetrical inductive window at the cross section where the rectangular guide intersects the circular guide. The septum is slideable along the axis of the circular guide and is perpendicular to the plane of symmetry. The coupling is achieved by properly selecting the width of the iris opening and adjusting the position of the septum. Trimming is done by the tuning screws which are introduced into each guide in the region where the electric field is a maximum.

The tuning of the junction may be accomplished with a short pulse set. The set in use is capable of sending a short pulse with carrier 11.2 Gc/s into the component under test and then displaying simultaneously on a scope the return pulses reflected from various discontinuities separated in proper sequence by time differences proportional to physical distances between the discontinuities. When tuning, the rod is placed parallel to the axis of the guide in the plane of symmetry, Fig. 4, making cutoff frequency at every cross section the same as that at the entrance of the equalizer. This placement of the rod gives rise to two distinctly separated return pulses on the scope, the first being reflected from the junction followed by the second being reflected from the end of the equalizer. Choice of the width of the iris opening, positioning of the septum, and adjustments of the screws will then be made to minimize the magnitude of the reflected pulse from the junction, i.e., to maximize the power coupled into the circular guide. Since the power coupling depends upon the cutoff frequency at the entrance of the equalizer, the junction should be tuned for a specific entrance cutoff frequency. For example, Fig. 5 shows the magnitudes of pulses reflected from the junction after tuning for various cutoff frequencies at

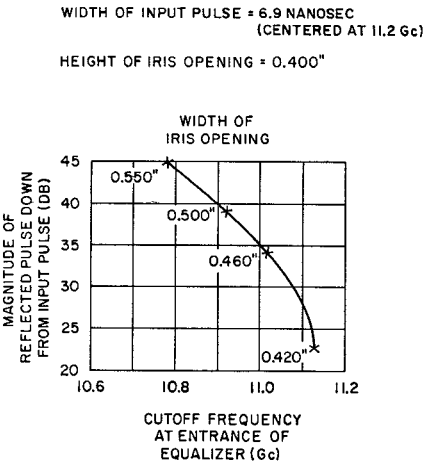

Fig. 5. Magnitude of reflected pulse from input junction after tuning for various cutoff frequencies at entrance of equalizer.

the entrance of the equalizer when an input pulse of 6.9 ns centered at 11.2 Gc/s is being used. The reflections are smaller at lower entrance cutoff frequencies since the center frequency of the input pulse is farther above cutoff.

After the junction has been tuned, the rod is put back to its intended orientation to produce the desired tapering effect for the equalizer. Final adjustments of the screws will then be made to improve the delay vs. frequency characteristic.

V. Results

The theoretical delay characteristic of the equalizer when the axis of the slanted rod is straight is calculated in Appendix II. The actual performance has been measured by a delay measuring set [5] capable of providing direct display of delay vs. frequency characteristic on a scope or on an X-Y recorder. The measured bandwidth and center frequency are as predicted. The average of the measured delay characteristic checks approximately with the theory except in the region near the low frequency end of the band as shown in Fig. 6. The deviation is due to the combined effect of 1) the presence of the tuning screws, which not only tunes the junction but also perturbs the dimensions of the input (low frequency) region of the equalizer, 2) the lack of straightness of the guide and the rod, and 3) the abrupt ending of the taper at the end of the equalizer.

When the rod is stretched and locked at both ends of the guide in a given orientation, the shape of the delay characteristic can be altered by deflecting the axis of the rod. The rod axis may be deflected into different curvatures by pulling some or all of the threads in varying amounts. Upon properly shaping the curvature of the rod axis, various delay characteristics have been obtained as shown in Figs. 7 and 8. In particular, Fig. 8 represents an equalizer capable of providing a total differential linear delay of 44.6 ns over a band of 680 Mc/s (10.80 to 11.48 Gc/s), which is more than sufficient to

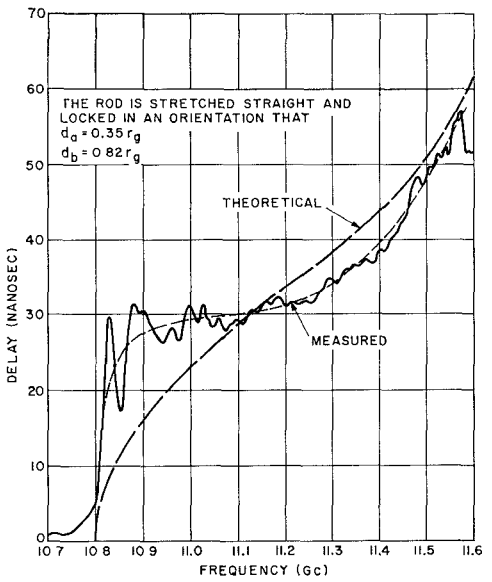

Fig. 6. Theoretical and measured delay characteristics of a slanted-rod delay equalizer. $r_r = 0.0545$ inch, $r_g = 0.309$ inch, $L = 59.5$ inches.

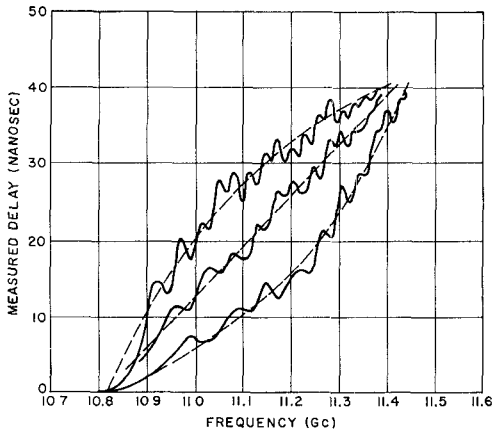

Fig. 7. Various delay characteristics obtained upon shaping the axis of the rod in the equalizer of Fig. 6.

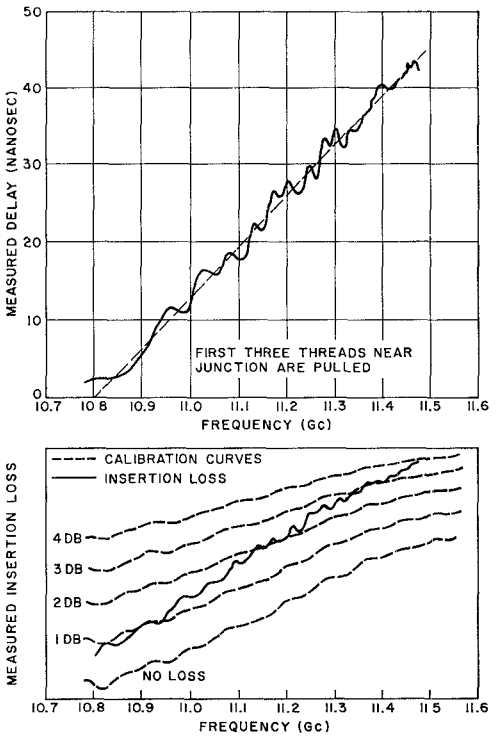

Fig. 8. Delay and insertion loss characteristics after the axis of the rod in the equalizer of Fig. 6 being shaped for linear delay.

provide, for example, the 23 ns differential linear delay over a band of 500 Mc/s required for equalizing the delay distortion at 50 Gc/s introduced by the section of 2-inch ID circular guide between repeaters 20 miles apart. The delay characteristic shows a maximum of about 2.4 ns deviation from linearity. This deviation may be improved by reducing reflections from the input junction and by more discreet shaping of the rod axis. The measured insertion loss rises from about 0.6 dB at the low frequency end of the band to about 3.8 dB at the high frequency end. The loss is attributed to 1) large attenuation near cutoff on account of imperfect conducting boundaries, and 2) absorption by the matched load resulting from wave penetration beyond the cutoff cross section.

The bandwidth, center frequency, and total available, delay of the equalizer can be varied by varying the rod orientation or by changing the rod size as illustrated by the theoretical delay characteristics in Figs. 9, 10, and 11. Each curve in these figures corresponds to a rod orientation defined by the positions of the rod d_a and d_b at the entrance and the end of the equalizer. The delay τ is plotted as a function of f/f_{cq}, the signal frequency normalized with respect to the cutoff frequency of the guide.

The experiments done so far show that the perturbation theory (assuming $r_r \ll r_g$) for slanted-rod delay equalizers is valid for ratio of rod radius to guide radius

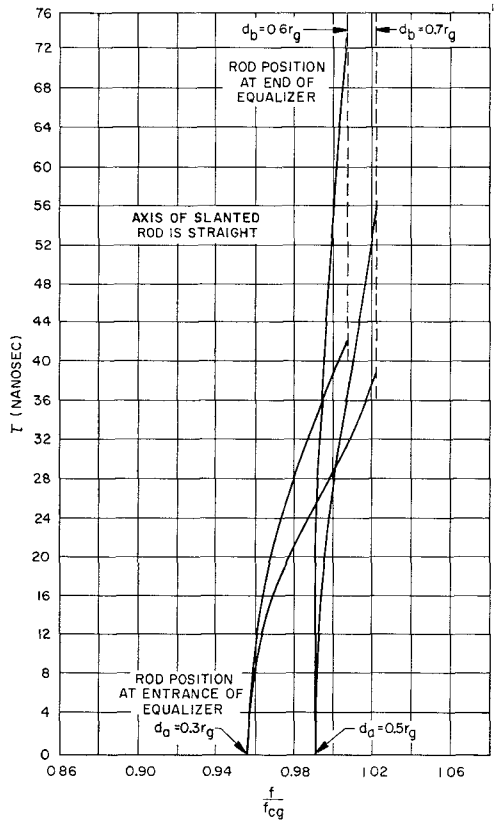

Fig. 9. Theoretical delay characteristics. $r_r/r_g = 0.176$, $L = 1$ m.

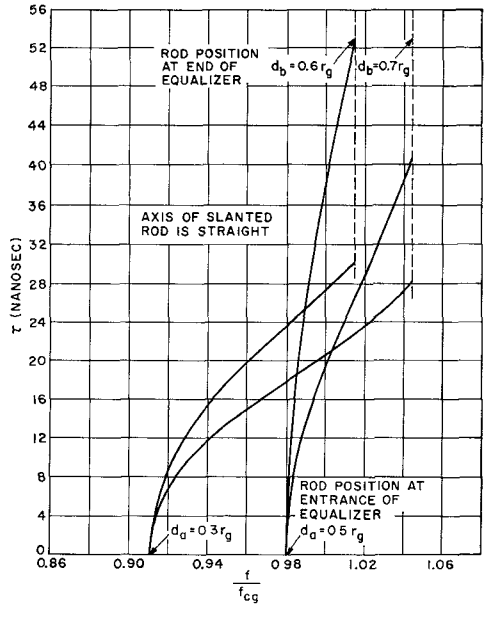

Fig. 10. Theoretical delay characteristics. $r_r/r_g = 0.250$, $L = 1$ m.

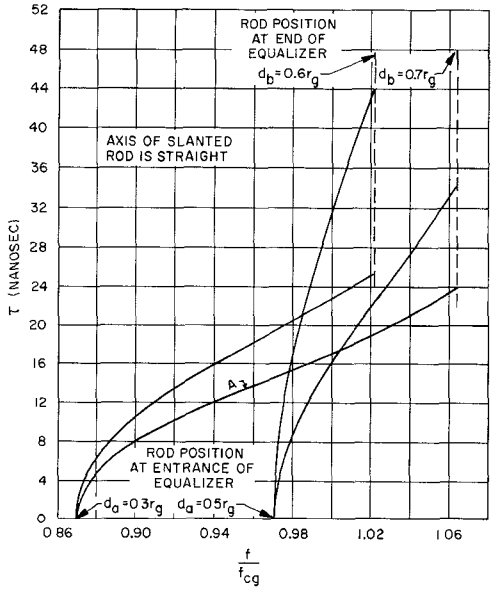

Fig. 11. Theoretical delay characteristics. $r_r/r_g = 0.300$, $L = 1$ m.

of 0.176. Admitting that the theory still holds for ratio 0.3, it is then possible to use this structure for much wider bandwidths. For instance, curve A in Fig. 11 indicates that a slanted-rod delay equalizer 1 m long may provide a total delay of 24 ns over a band of 2.24 Gc/s at 11.2 Gc/s.

Since parameters and abscissas are normalized, the theoretical characteristics can be used to estimate the performances of slanted-rod delay equalizers at other frequencies. For instance, from curve A in Fig. 11 one deduces that a total delay of 24 ns over a band of 1.2 Gc/s at 6 Gc/s may be achieved with a structure 1 m long provided that: $r_r = 0.3r_g$, $d_a = 0.3r_g$, $d_b = 0.7r_g$, and $r_g = 0.0142$ m.

VI. Conclusions and Suggestions

Based on the results obtained, the new model of microwave delay equalizer demonstrates the following:

1) It can provide large amounts of delay over wide bands at microwave frequencies. Theoretical estimations show that at 11.2 Gc/s a total delay of 24 ns over a band of 2.24 Gc/s may be achieved with a structure 1 m long, and at 6 Gc/s the same delay over a band of 1.2 Gc/s may be achieved with a structure 1 m long.
2) It provides adjustable performance. The bandwidth, center frequency, and total available delay can be varied by varying the rod orientation or by changing the rod size. The shape of delay characteristic can be varied by shaping the rod axis.
3) It can be used to equalize the delay distortion introduced by the section of waveguide between adjacent repeaters in the proposed 35–75 Gc/s, TE_{01} mode, 2-inch ID circular waveguide transmission system. Experimental results show that a linear delay of the order of 45 ns over a band of 680 Mc/s (10.80 to 11.48 Gc/s) can be obtained with a structure 1.5 m long. This is more than sufficient to provide, for example, the 23 ns linear delay over a band of 500 Mc/s required at 50 Gc/s for repeaters 20 miles apart.
4) It can also be used to equalize delay distortions introduced by other parts of the system besides the circular waveguide. Delay characteristics other than linear can be obtained by properly shaping the rod axis.

The following are some suggestions for improvement when this model is to be developed for practical use in the system:

1) The supporting and deflecting mechanisms of the rod should be redesigned so that continuous varying of the rod orientation and finer shaping of the rod axis are possible.
2) A better way of maintaining rod positions in the guide after shaping the rod axis, other than using the tension of the threads, should be devised for rigidity and permanency, such as filling the guide with dielectric.
3) Reflections at the input junction should be reduced in order to diminish the ripples in the delay characteristics as shown in Figs. 7 and 8.

List of Principal Symbols

c Velocity of light in free space, $3 \cdot 10^8$ ms
d Distance between center of rod and center of circular guide
d_a Distance between center of rod and center of circular guide at entrance (low frequency end) of equalizer
d_b Distance between center of rod and center of circular guide at end (high frequency end) of equalizer
F Elliptic integral of the first kind
f Signal frequency
f_a Cutoff frequency at entrance (low frequency end) of equalizer
f_{a1} Cutoff frequency of perturbed circular guide when center of rod is located at center of guide
f_b Cutoff frequency at end (high frequency end) of equalizer
f_{b1} Cutoff frequency of perturbed circular guide when center of rod is located at wall of guide
f_c Cutoff frequency
f_{cg} Cutoff frequency of circular guide
J_n Bessel function of the first kind, nth order
J_n' Derivative of J_n with respect to its argument
K Complete elliptic integral of the first kind
L Length of taper or equalizer
r_r Radius of rod
r_g Inner radius of circular guide
z Axial coordinate
z_0 Location of cross section in z coordinate where cutoff frequency of taper or equalizer is equal to signal frequency
ξ Normalized axial coordinate, z/L
ξ_0 Location of cross section in ξ coordinate where cutoff frequency of taper or equalizer is equal to signal frequency
ρ Radial coordinate of cylindrical coordinate system
τ Delay of frequency f
ϕ Angular coordinate of cylindrical coordinate system

Appendix I

The cutoff frequency of a circular waveguide perturbed by a metallic rod is derived in this appendix following Szentirmai's method [6]. The derivation is based on these assumptions:

1) The wave energy is in the TE_{11} mode propagating in the axial (z) direction.
2) The rod is in the plane of symmetry.
3) The diameter of the rod is much smaller than that of the guide.
4) The guide and the rod are lossless.

When the rod is in the plane of symmetry and parallel to the axis of the guide as shown in Fig. 12, the scalar function u, representing the axial component of the magnetic field, must satisfy the two-dimensional wave equation

$$(\nabla^2 + \beta_c^2)u = 0, \tag{1}$$

and the condition that its normal derivative is zero, i.e.,

$$\frac{\partial u}{\partial n} = 0 \tag{2}$$

on the boundary of the guide B_g and on the boundary of the rod B_r. In the process of solving u from (1) and

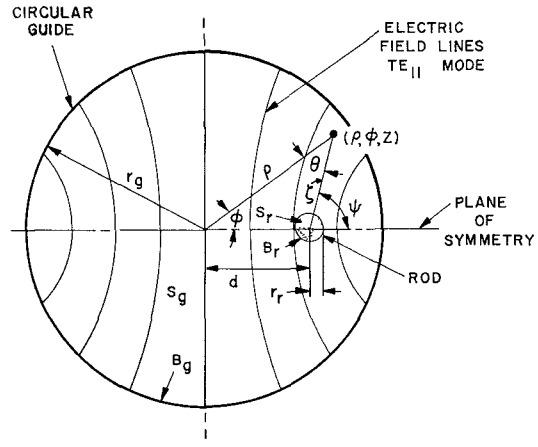

Fig. 12. Perturbation of a circular guide by a metallic rod.

(2), the cutoff wave number β_c is uniquely determined for each mode. The cutoff frequency of the perturbed guide is related to β_c by

$$f_c = \frac{c}{2\pi}\beta_c \tag{3}$$

where c is the velocity of light in free space.

Similarly, when the rod is absent from the guide, the scalar function v must satisfy

$$(\nabla^2 + \beta_{cg}^2)v = 0 \tag{4}$$

and the boundary condition

$$\frac{\partial v}{\partial n} = 0 \tag{5}$$

on B_g. The solution for this unperturbed case is known to be, in terms of the radial ρ and angular ϕ coordinates of the cylindrical coordinate system,

$$v = v_0 J_1(\beta_{cg}\rho)\cos\phi \tag{6}$$

with

$$\beta_{cg} r_g = 1.841, \tag{7}$$

where v_0 is a constant. The cutoff frequency of the unperturbed guide is given by

$$f_{cg} = \frac{1.841}{2\pi}\frac{c}{r_g}. \tag{8}$$

By utilizing (6) and (7), the cutoff wave number β_c and hence the cutoff frequency f_c of the perturbed case may be determined without actually having to solve (1) and (2). Applying Green's theorem, we have

$$\iint_{S_g - S_r}(v\nabla^2 u - u\nabla^2 v)ds = \int_{B_g + B_r}\left(v\frac{\partial u}{\partial n} - u\frac{\partial v}{\partial n}\right)dl \tag{9}$$

where S_g is the area enclosed by B_g, and S_r is the area enclosed by B_r. The surface integral is evaluated over the area between the boundaries of the guide and the rod. The line integral is evaluated along the boundaries of the guide and the rod. On account of (1), (2), (4), and (5), we simplify (9) to

$$(\beta_c^2 - \beta_{cg}^2)\iint_{S_g - S_r} uvds = \int_{B_r} u\frac{\partial v}{\partial n}dl. \tag{10}$$

Since S_r is negligible in comparison with S_g and u is essentially v except in the vicinity of the rod, the surface integral on the left side of (10) may be approximated by

$$\iint_{S_g - S_r} uvds \doteq \iint_{S_g} v^2 ds. \tag{11}$$

Substituting (6) into (11) and performing the integration gives

$$\iint_{S_g - S_r} uvds \doteq v_0^2\frac{\pi r_g^2}{2}\left[J_1^2(\beta_{cg}r_g) - J_0^2(\beta_{cg}r_g)\right]. \tag{12}$$

The line integral on the right side of (10) may be evaluated by a change of coordinates. Referring to Fig. 12, we have

$$\rho\cos\theta = \zeta + d\cos\psi \tag{13}$$

$$\rho\sin\theta = d\sin\psi. \tag{14}$$

The line integral becomes, in terms of ζ and ψ,

$$\int_{B_r} u\frac{\partial v}{\partial n}dl = -\int_{-\pi}^{+\pi}\left[u\frac{\partial v}{\partial \zeta}\right]_{\zeta = r_r} r_r d\psi. \tag{15}$$

To obtain the expression for v in terms of the new coordinates, we expand $v_0 J_1(\beta_{cg}\rho)e^{j\phi}$ in series and then take the real part. Utilizing the integral representation of the Bessel function of the first kind [7], we have

$$v_0 J_1(\beta_{cg}\rho)e^{j\phi} = \frac{v_0}{2\pi j}\int_0^{2\pi} e^{j[\Omega+\theta+\phi+\beta_{cg}\rho\cos(\Omega+\theta)]}d\Omega. \tag{16}$$

The angle θ can be arbitrarily added since the integrand is periodic in Ω. After trigonometric manipulations, (16) becomes

$$v_0 J_1(\beta_{cg}\rho)e^{j\phi} = \frac{v_0}{2\pi j}\int_0^{2\pi} e^{j[\Omega+\psi+\beta_{cg}d\cos(\Omega+\psi)+\beta_{cg}\zeta\cos\Omega]}d\Omega. \tag{17}$$

Using the series expansion [8]

$$e^{j\beta_{cg}d\cos(\Omega+\psi)} = \sum_{m=-\infty}^{\infty} j^m J_m(\beta_{cg}d)e^{jm(\Omega+\psi)} \tag{18}$$

in (17), performing the integration, and then taking the real part, we find

$$v = v_0\sum_{m=-\infty}^{\infty}(-1)^m J_m(\beta_{cg}d)J_{m+1}(\beta_{cg}\zeta)\cos(m+1)\psi. \tag{19}$$

In the region around the rod $\zeta \ll r_g$. Expanding $J_{m+1}(\beta_{cg}\zeta)$ in power series and neglecting high powers of $\beta_{cg}\zeta$ yields

$$v = v_0\left[J_1(\beta_{cg}d) + \zeta\beta_{cg}J_1'(\beta_{cg}d)\cos\psi - \zeta^2\beta_{cg}^2\frac{J_1(\beta_{cg}d) + J_2'(\beta_{cg}d)\cos 2\psi}{4} + \cdots\right], \quad \zeta \ll r_g. \tag{20}$$

For the expression of u, we assume

$$u = \sum_{i=0}^{\infty} b_i(\psi)\zeta^i \left[1 + \frac{r_r^2}{\zeta^2}\right]^i \tag{21}$$

which satisfies the boundary condition stated by (2). Since u is essentially v when $\zeta \gg r_r$, we determine $b_i(\psi)$'s by neglecting r_r^2/ζ^2 in the bracket of (21) and then equating the coefficients of the powers of ζ with those of (20) respectively. Thus

$$u = v_0\left[J_1(\beta_{cg}d) + \zeta\left(1 + \frac{r_r^2}{\zeta^2}\right)\beta_{cg}J_1'(\beta_{cg}d)\cos\psi + \cdots\right], \qquad \zeta \ll r_g. \tag{22}$$

Substitute (20) and (22) into (15) and integrate, yielding

$$\int_{B_r} u\frac{\partial v}{\partial n}dl \doteq -v_0^2\pi\beta_{cg}^2 r_r^2 \cdot [2J_1'^2(\beta_{cg}d) - J_1^2(\beta_{cg}d)]. \tag{23}$$

Substituting (12) and (23) into (10) and then utilizing (3), (7), and (8) gives the cutoff frequency of the perturbed guide as

$$f_c = f_{cg}\left\{1 + 8.379\left(\frac{r_r}{r_g}\right)^2 \cdot\left[J_1^2\left(1.841\frac{d}{r_g}\right) - 2J_1'^2\left(1.841\frac{d}{r_g}\right)\right]\right\}^{1/2}. \tag{24}$$

It may easily be shown from (24) that 1) f_c is equal to f_{cg} when d is equal to $0.557r_g$, 2) f_c becomes gradually lower than f_{cg} as d decreases from that value, and 3) f_c becomes gradually higher than f_{cg} as d increases from that value. Since the cutoff frequency is inversely related to the effective cross section of the perturbed guide, (24) substantiates the general results outlined in Section II.

The right side of (24) may be approximated by a simpler expression as follows. Define f_{a1} and f_{b1} as the cutoff frequencies of the perturbed guide when the center of the rod is located at the center and at the wall of the guide, respectively. Setting d in (24) equal to zero and r_g, respectively, we have

$$f_{a1} = f_{cg}\sqrt{1 - 4.189\left(\frac{r_r}{r_g}\right)^2} \tag{25}$$

$$f_{b1} = f_{cg}\sqrt{1 + 2.837\left(\frac{r_r}{r_g}\right)^2} \tag{26}$$

where f_{cg} is given by (8). From (24), (25), and (26), we obtain

$$\frac{f_c^2 - f_{a1}^2}{f_{b1}^2 - f_{a1}^2} = 0.5963 + 1.193 \cdot\left[J_1^2\left(1.841\frac{d}{r_g}\right) - 2J_1'^2\left(1.841\frac{d}{r_g}\right)\right] \tag{27}$$

Figure 13 shows that the right side of (27) may be replaced by $\sin^2(\pi/2)(d/r_g)$ with remarkable accuracy.

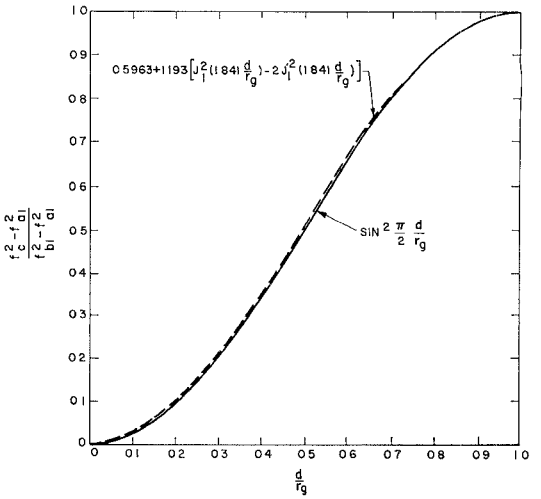

Fig. 13. Plot of $(f_c^2-f_{a1}^2)/(f_{b1}^2-f_{a1}^2)$ as a function of normalized rod position.

Hence, a good approximation for the cutoff frequency of the perturbed guide is, from (27),

$$f_c \doteq \left\{(f_{b1}^2 - f_{a1}^2)\sin^2\frac{\pi}{2}\frac{d}{r_g} + f_{a1}^2\right\}^{1/2} \tag{28}$$

in which f_{a1} and f_{b1} are given by (25) and (26).

Appendix II

The theoretical delay characteristic of an equalizer in which the taper is simulated by slanting a straight metallic rod in an otherwise uniform circular guide is derived here under the same assumptions as outlined in Appendix I.

Referring to Fig. 14, the signal of frequency f enters a waveguide taper, undergoes cutoff reflection and then returns to the entrance of the taper. For simplicity, consider the ideal case that the signal is totally reflected at z_0, the location of the cross section at which the cutoff frequency of the taper becomes equal to the signal frequency. The total phase change Φ of the signal during the round trip is then

$$\Phi = 2\int_0^{z_0}\beta(z)dz \qquad 0 \le z_0 \le L, \tag{29}$$

where $\beta(z)$ is the propagation constant given by

$$\beta(z) = \frac{2\pi}{c}\sqrt{f^2 - f_c^2(z)}. \tag{30}$$

Using the basic definition

$$\tau = \frac{1}{2\pi}\frac{d\Phi}{df} \tag{31}$$

together with (29) and (30) the delay experienced by the signal during the round trip may be expressed as

$$\tau = \frac{2}{c}f\int_0^{z_0}\frac{dz}{\sqrt{f^2 - f_c^2(z)}}. \tag{32}$$

Upon introducing the normalized axial coordinate

$$\xi = \frac{z}{L} \tag{33}$$

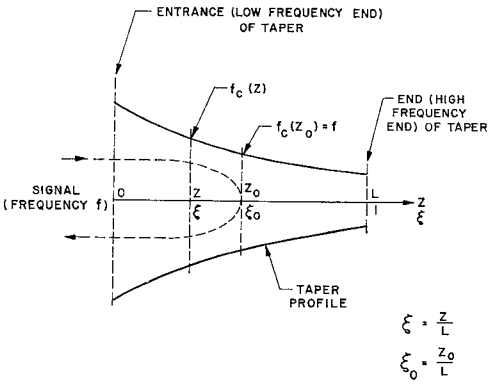

Fig. 14. Cutoff reflection in a waveguide taper

the delay is

$$\tau = \frac{2L}{c} f \int_0^{\xi_0} \frac{d\xi}{\sqrt{f^2 - f_c^2(\xi)}} \qquad 0 \le \xi_0 \le 1. \quad (34)$$

For an equalizer in which the taper is simulated by slanting a metallic rod in an otherwise uniform circular guide, the cutoff frequency at any cross section is given approximately by (28) in terms of the distance between the center of the rod and the center of the guide at the same cross section. When the axis of the slanted rod is straight, the following relationship exists, from Fig. 2,

$$\frac{d}{r_g} = \frac{d_a}{r_g} + \frac{d_b - d_a}{r_g} \xi \quad (35)$$

where d_a and d_b are the distances between the center of the rod and the center of the guide at the entrance and at the end of the equalizer respectively. Substitution of (35) into (28) gives the cutoff frequency in terms of the axial coordinate as

$$f_c(\xi) = \left\{ (f_{b1}^2 - f_{a1}^2) \cdot \sin^2 \frac{\pi}{2} \left[\frac{d_a}{r_g} + \frac{d_b - d_a}{r_g} \xi \right] + f_{a1}^2 \right\}^{1/2}. \quad (36)$$

It follows that the cutoff frequency at the cross section where reflection takes place is

$$f_c(\xi_0) = \left\{ (f_{b1}^2 - f_{a1}^2) \cdot \sin^2 \frac{\pi}{2} \left[\frac{d_a}{r_g} + \frac{d_b - d_a}{r_g} \xi_0 \right] + f_{a1}^2 \right\}^{1/2}. \quad (37)$$

At this location the signal frequency is equal to the cutoff frequency. Replacing $f_c(\xi_0)$ in (37) by f and then solving for ξ_0, we obtain

$$\xi_0 = \frac{r_g}{d_b - d_a} \left[\frac{2}{\pi} \sin^{-1} \sqrt{\frac{f^2 - f_{a1}^2}{f_{b1}^2 - f_{a1}^2}} - \frac{d_a}{r_g} \right]. \quad (38)$$

Using (34), (36), and (38), the delay characteristic of the equalizer may be evaluated from

$$\tau = \frac{2L}{c} \frac{f}{\sqrt{f^2 - f_{a1}^2}} \cdot \int_0^{\xi_0} \frac{d\xi}{\sqrt{1 - \frac{f_{b1}^2 - f_{a1}^2}{f^2 - f_{a1}^2} \sin^2 \frac{\pi}{2} \left[\frac{d_a}{r_g} + \frac{d_b - d_a}{r_g} \xi \right]}} \qquad 0 \le \xi \le 1. \quad (39)$$

Performing the integration, the delay is

$$\tau = \frac{4L}{\pi c} \frac{r_g}{d_b - d_a} \frac{f}{\sqrt{f_{b1}^2 - f_{a1}^2}} \left\{ K \left[\sqrt{\frac{f^2 - f_{a1}^2}{f_{b1}^2 - f_{a1}^2}} \right] - F \left[\sqrt{\frac{f^2 - f_{a1}^2}{f_{b1}^2 - f_{a1}^2}}, \sin^{-1} \frac{\sin \frac{\pi}{2} \frac{d_a}{r_g}}{\sqrt{\frac{f^2 - f_{a1}^2}{f_{b1}^2 - f_{a1}^2}}} \right] \right\} \quad (40)$$

where F is the elliptic integral of the first kind and K is the complete elliptic integral of the first kind.

To locate the operating band, the cutoff frequencies at the entrance and the end of the equalizer f_a and f_b are required. Upon replacing ξ in (36) by zero and one respectively, the cutoff frequency at the entrance is

$$f_a = \left\{ (f_{b1}^2 - f_{a1}^2) \sin^2 \frac{\pi}{2} \frac{d_a}{r_g} + f_{a1}^2 \right\}^{1/2} \quad (41)$$

and the cutoff frequency at the end is

$$f_b = \left\{ (f_{b1}^2 - f_{a1}^2) \sin^2 \frac{\pi}{2} \frac{d_b}{r_g} + f_{a1}^2 \right\}^{1/2}. \quad (42)$$

The difference of $f_b - f_a$ gives the bandwidth of the equalizer.

The theoretical delay given by (40) has been computed for different rod orientations and for different rod sizes. The results are shown in Figs. 9, 10, and 11. The delay contributed by the short piece of rectangular guide at the input of the equalizer has been neglected.

Acknowledgment

The author is indebted to E. A. Marcatili for helpful suggestions, to W. D. Warters for making available the short pulse set, and to C. L. Beattie for assistance in the computations.

References

[1] Miller, S. E , Waveguide as a communication medium, *Bell Sys. Tech. J.*, vol 33, Nov 1954, pp 1209–1265.
[2] Pierce, J. R., Tapered wave guide delay equalizer, U. S. Patent No. 2,863,126, Dec 1958.
[3] Tang, C. C. H., Delay equalization by tapered cutoff waveguides, *IEEE Trans. on Microwave Theory and Techniques*, vol MTT-12, Nov 1964, pp 608–615.
[4] Mumford, W. W., Electromagnetic wave equalization, U. S. Patent No. 2,767,379, Oct 1956.
[5] Chinnock, E. L., Direct reading sweep frequency microwave delay measuring set, to be published.
[6] Szentirmai, G., private communication.
[7] Jahnke, E., and F. Emde, *Table of Functions*. N. Y.: Dover, 1945, p 149.
[8] Erdélyi, A., W. Magnus, F. Oberhettinger, and F. G. Tricomi, *Higher Transcendental Functions*, vol 2. N. Y.: McGraw-Hill, 1953, p 7.